Bi-penalty stabilized technique with predictor-corrector time scheme for contact-impact problems of elastic bars

Radek Kolman[a,*], Ján Kopačka[a], José A. González[b], S.S. Cho[c], K.C. Park[d]

[a] *Institute of Thermomechanics of the CAS, v. v. i., Dolejškova 1402/5, 182 00 Praha 8, Czech Republic*
[b] *Escuela Técnica Superior de Ingeniería, Universidad de Sevilla, Camino de los Descubrimientos s/n, Seville E-41092, Spain*
[c] *Reactor Mechanical Engineering Devision, Korea Atomic Energy Research Institute, 999-111 Daedeok-Daero, Yuseong-gu, Daejeon 305-353, Republic of Korea*
[d] *Department of Aerospace Engineering Sciences, University of Colorado at Boulder, CO 80309-429, USA*

Abstract

This paper deals with a stabilization technique for the finite element modelling of contact-impact problems of elastic bars via *bi-penalty method*. We employ the finite element method with explicit time integration and the penalty method for enforcement of contact constraints. The bi-penalty method is a modification of the classical penalty method adding a new mass penalized term which is able to maintain the critical time step of the contact-free problem. To suppress spurious oscillations in the contact forces and increase the overall stability of the contact-impact algorithm, it is proposed to combine the bi-penalty method with a predictor-corrector stabilized explicit time integration scheme. Moreover, these oscillations are attenuated for a wide range of the stiffness penalty parameter, provided that the optimal bi-penalty ratio is preserved. For time integration, the standard central difference method, its stabilized version and Park time scheme are employed. Also, different mass matrices are tested with an optimal setting given by the ratio of mass and stiffness penalized matrices. It is shown that this optimal ratio can be set with respect to the maximum eigen-frequency of finite elements in contact constraints. The methodology is tested for one-dimensional contact-impact problems – the Signorini problem and impact of two elastic bars with different length.

Keywords: Finite element method, explicit integration, contact-impact problems, penalty method, bi-penalty method, stability analysis

1. Introduction

Obtaining fast, stable and accurate solutions of contact-impact problems remain at the forefront of computational mechanics research. Applications in this field appear in real-world problems from mechanical and civil engineering, bio-mechanics, ballistics, or aviation and aerospace engineering. In this paper, we

*Corresponding author
Email addresses: kolman@it.cas.cz (Radek Kolman), kopacka@it.cas.cz (Ján Kopačka), japerez@us.es (José A. González), sscho96@kaist.ac.kr (S.S. Cho), kcpark@colorado.edu (K.C. Park)

focus on the finite element modelling of contact-impact problems of elastic bars under the linear deformation theory without damping. In the space discretization, linear finite elements and the consistent, lumped, and averaged mass matrices are employed. Attention is paid only to the explicit time integration with a constant time step and its stability. For contact constraints enforcement, the classical stiffness penalty method and the bi-penalty modification are considered.

Most frequently, penalty methods, Lagrange multipliers method, its localized variant and augmented Lagrangian methods are applied for modelling dynamic contact problems in the context of the finite element analysis, e.g. see [1, 2, 3, 4]. In explicit finite element analysis, the penalty method is preferred due to its implementation simplicity and fast evaluation of contact forces [1] which, in comparison to Lagrange Multipliers method, does not increase the number of unknowns. It is also needed to mention the works related to efficient active set approaches in contact problems as [5, 6]. On the other hand, the main disadvantage of the penalty method in elastodynamics is the fact that the stability limit of the explicit time integration scheme is destroyed by a large value of the numerical stiffness penalty parameter used for contact constraints enforcement [1]. The stable time step size rapidly decreases with increasing value of the penalty stiffness parameter as is depicted in Fig. 1.

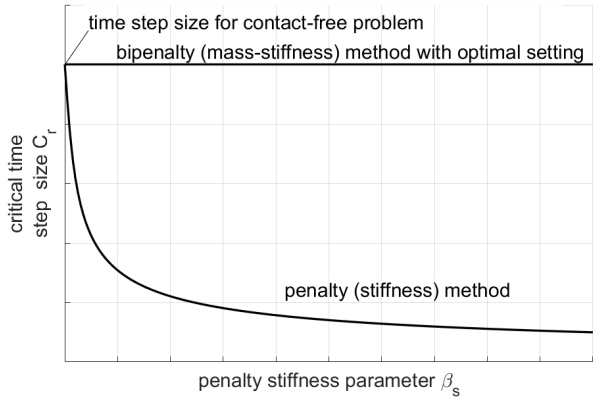

Figure 1: Characteristic dependence of the stable time step size for the penalty and bi-penalty methods with optimal setting. In the penalty method, the stable time step size is strongly affected by the penalty stiffness parameter β_s while bi-penalty with optimal setting remains unaffected.

A complete review of time integration strategies for contact-impact/dynamic contact problems in finite element modelling can be found in [7]. In general, one can use implicit or explicit time integration schemes. In this paper, we focus only on explicit time integration. For examples, the implicit time schemes have been applied in impact-contact problems in [8, 9, 4, 10, 11, 12]. On the other hands, the explicit time schemes for the contact-impact problems have been employed in [13, 14, 1, 2, 15, 16]. The explicit-implicit time scheme in contact-impact problems has been adopted in [17]. The explicit predictor-corrector algorithm has been

designed for dynamic contact with smooth and non-smooth surface geometries in [18].

Moreover, it is well known that the results of contact problems modelled via the penalty-like methods depend on the used value of the penalty parameter. The principle of the penalty method implies that impenetrability conditions are always met only approximately. With a higher value of the penalty parameter, more precise fulfilment of the impenetrability conditions occurs. We know that penalty methods are generally not consistent [7] within the variational formulation of the problem and the final matrix form is ill-conditioned. Often, the solution of the contact problem depends on the penalty parameters and the convergence to the correct solution is not guaranteed [7]. A direct consequence of only approximate fulfilment of the contact constraints is a non-zero penetration, which causes the contact term to produce non-physical energy corresponding to the contact interfaces. A good solution to the oscillations on contact forces is the application of time schemes based on predictor and corrector phases for evaluating kinematical quantities. The regularization of the penalty approach in the finite element method of the impact of elastic bars is presented in Otto's work [19] and extension to the spectral 3D finite element method with NURBS contact tying for contact surfaces is published in [20]. In these works, the nonlinear penalty stiffness parameter is employed with explicit Runge-Kutta time integration of order 4. In this field, it is also important to mention the works of C. Felippa [21, 22, 23].

Also, during the convergence process, final penetration is not exactly zero as corresponds to contact non-penetration condition. As a consequence, there is lost energy included in the penalty contact term, which is not a physical one and it is a product of numerical behaviour of the method. One way to eliminate this undesired numerical effect is to use the bi-penalty method [24]. In Fig. 1, the effect on the stability limit of the penalty method is shown, as well as the optimal setting for the bi-penalty method, for details see [24, 25].

In the bi-penalty method, an extra mass term is added into the mass distribution corresponding to a contact domain of interest with a stiffness term at the same time as in the classical penalty method. This modification of the penalty method is known from Asano [26] and later from Armero [10]. Excellent progress and different applications to several problems have been made by Hetherington [27, 28, 24]. The penalty based method in multibody dynamics is also a well-known technique for stabilization of constraints, for example, see the Park's method [29] and Baumgarte's method [30]. In this area, the bi-penalty or tri-penalty modification is a common technique used for stabilization of oscillations in the constraints connecting the bodies. In numerical analysis, the bi-penalty method is known as the *consistent penalty method*, see [31].

Another important problem in the numerical modelling of contact-impact problems comes from spurious oscillations of contact forces, often caused by activation and deactivation (zig-zag effect) of contact constraints during the solution process. A lot of numerical techniques and strategies have been proposed in the literature for elimination and stabilization of spurious oscillations in the contact forces. One can mention the work of Doyen [32], the stabilized implicit Newmark method for non-smooth dynamics and contacts [17, 33],

mass redistribution techniques [34], singular mass techniques [35, 36] or the stabilized explicit scheme with the penalty method [37]. The last mentioned technique can be also applied in connection with the bi-penalty method for stabilization of spurious oscillations of contact forces.

In this paper, we present an explicit time integration scheme for finite element solution of contact-impact problems based on the central difference method [38], in particular, its stabilized version using the predictor-corrector approach [7, 37] and Park explicit time scheme with predictor-corrector stabilization of contact forces [39] in combination with the bi-penalty formulation [25]. Superior behaviour of the presented method for modelling contact-impact problems is demonstrated using the impact problem of elastic bars and the Signorini problem. The obtained results are compared with the standard time integration scheme used in explicit finite element procedures for impact-contact problems, the central difference method [38]. It is observed, the standard explicit central difference method is not able to integrate accurately in time the wave propagation problem with a time step size smaller than the stability limit. It is known that only the combination in explicit time integration via the central difference method on the uniform linear finite element mesh, with lumped mass matrix and time step corresponding to the critical time step size in a uniform gives exact results of wave propagation. Otherwise, the results are polluted by spurious stress oscillations, provided that the time step size is smaller than the stability limit. Park explicit time scheme [39] is able to track a wavefront eliminating the effect of time step size on accuracy so it is a suitable tool for modelling contact-impact problems.

The paper is organized as follows. In Section 2, the governing equations for impact of elastic bars with the definition of the gap function for contact interfaces are presented and introduced with strong and weak forms. In Section 3, the finite element discretized equations for the motion of elastic bars with the bi-penalty method are derived. The explicit time integration of contact-impact problems in the finite element method is presented in Section 4 together with the stability limit. Also, the optimal setting for the penalty mass matrix is derived. Results for numerical tests in one-dimensional case – the Signorini and Huněk tests – are presented in Section 5 with comments on the behaviour and superior properties of the proposed methodology. The paper closes with the conclusions in Section 6.

2. Formulation of the contact problem and governing equations

In this section, we define the strong and weak formulations of the impact-contact problem for elastic bars, including the definition of a gap function to enforce the contact constraints with the bi-penalty method. In the following, we assume that the elastic bars in contact are homogeneous with the same constant cross-section A, Young modulus E and mass density ρ. The lengths are different for each bar as well as their initial velocities of v_{i0}.

2.1. Strong formulation of contact initial-boundary value problem in 1D

The correct mathematical formulation of the dynamic contact problems including the impenetrability condition as well as the persistency condition is presented in [8]. The one-dimensional contact-impact problem for linear isotropic homogeneous bars is governed by the following constrained initial-boundary value problem (IBVP) [7]:

$$\begin{cases} Eu'' = \rho\ddot{u} & \text{in } \boldsymbol{I}\times\boldsymbol{T} \\ u(x,0) = u_0(x) & \text{in } \bar{\boldsymbol{I}} \\ \dot{u}(x,0) = v_0(x) & \text{in } \bar{\boldsymbol{I}} \\ u(x,t) = \bar{u}(x) & \text{on } \Gamma_u \\ Eu'(x,t) = \bar{\sigma}(x) & \text{on } \Gamma_\sigma \\ g(t) \le 0 & \text{on } \boldsymbol{\Gamma}_{\mathrm{c}}\times\boldsymbol{T} \\ p_{\mathrm{c}} \ge 0 & \text{on } \boldsymbol{\Gamma}_{\mathrm{c}}\times\boldsymbol{T} \\ g(t)p_{\mathrm{c}} = 0 & \text{on } \boldsymbol{\Gamma}_{\mathrm{c}}\times\boldsymbol{T} \\ \dot{g}(t) \le 0 & \text{on } \boldsymbol{\Gamma}_{\mathrm{c}}\times\boldsymbol{T} \\ \dot{g}(t)p_{\mathrm{c}} = 0 & \text{on } \boldsymbol{\Gamma}_{\mathrm{c}}\times\boldsymbol{T} \end{cases} \tag{1}$$

where $\boldsymbol{I} = \bigcup_i \boldsymbol{I}_i = (x_i^\ell, x_i^r)$; $i = 1,2$ is the union of intervals of spatial points $x_i \in \boldsymbol{I}_i \subset \mathbf{R}$ defining the contacting bodies (see Figure 2), and $\boldsymbol{T} = (0, t_{\mathrm{end}})$; $t_{\mathrm{end}} \in \mathbf{R}$ is the time interval. For one-bar contact problem with a rigid obstacle only one body is considered and $\boldsymbol{I} = \boldsymbol{I}_1$. In the first Eq. (1), which governs the balance of the linear momentum, $u(x,t) : \boldsymbol{I}\times\boldsymbol{T} \mapsto \mathbf{R}$ is the unknown displacement function, $E \in \mathbf{R}^+$ is Young's elasticity modulus, and $\rho \in \mathbf{R}^+$ is the mass density. The eighth condition in Eq. (1) is the classical KKT complementarity condition between gap $g(t)$and pressure p_{c}, requiring that surface forces exist only during actual contact ($g = 0$). The penultimate condition in Eq. (1) is termed the persistency condition. Note that for the sake of simplicity, the second partial derivative with respect to x is denoted by double prime, $(\bullet)''$, whereas the second partial derivative with respect to t by superimposed dots, $(\ddot{\bullet})$.

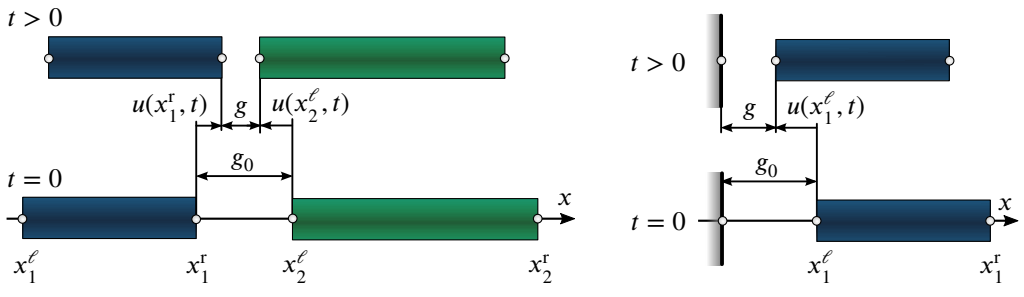

(a) two-bar contact (b) 1D Signorini problem

Figure 2: Definition of domains of interest, their boundaries and the gap function.

The governing equation $(1)_1$ is complement with the initial conditions $(1)_{2,3}$, Dirichlet and Neumann boundary conditions $(1)_{4,5}$, contact conditions $(1)_{6-8}$ and persistency condition $(1)_{9-10}$, where $g(t)$ and $\dot{g}(t)$ is the gap function and its rate defined in the following section and $p_c(t)$ is the contact pressure. In the initial conditions, $u_0(x) : \bar{\boldsymbol{I}} \mapsto \mathbf{R}$ is the initial displacement function and $v_0(x) : \bar{\boldsymbol{I}} \mapsto \mathbf{R}$ is the initial velocity function; both prescribed at time $t = 0$. Similarly for the boundary conditions, $\bar{u}(x) : \Gamma_u \mapsto \mathbf{R}$ is the displacement function and $\bar{\sigma}(x) : \Gamma_\sigma \mapsto \mathbf{R}$ is the traction function; both constant in time. Γ_u and Γ_σ are sets of boundary points where displacements and stresses are prescribed.

2.2. Definition of the gap function

Finally the contact constraints are prescribed by the Signorini-Hertz-Moreau conditions $(1)_{6-8}$, with the aid of the gap function, g, and contact pressure, p_c, on the set $\Gamma_\mathrm{c} = \{x_2^\mathrm{r}, x_1^\ell\}$. The contact pressure $p_\mathrm{c}(x,t) : \bar{\boldsymbol{T}} \mapsto \mathbf{R}$ is equal to $-Eu'$, assuming Hooke's law, and the gap function $g(t) : \bar{\boldsymbol{T}} \mapsto \mathbf{R}$ for the two-bar contact is defined as

$$g(t) = -\left[u(x_1^\ell, t) - u(x_2^\mathrm{r}, t) + g_0\right] \tag{2}$$

where g_0 denotes the initial gap, cf. Figure 2. For the one-bar contact the gap function can be considered as the special case of (4), assuming $x_2^\mathrm{r} = 0$ and $u(x_2^\mathrm{r}, t) = 0$

$$g(t) = -\left[u(x_1^\ell, t) + g_0\right] \tag{3}$$

According to this definition, the gap function has a positive sign in the case of penetration. Therefore, the inequality $(1)_6$ is called the impenetrability condition.

In the contact-impact problems, constraints on the normal components of the velocities of points in the contact are needed to include in the formulation. This condition is called the persistency condition. For 1D cases, the persistency condition can be prescribed via the gap rate as

$$\dot{g}(t) = -\left[\dot{u}(x_1^\ell, t) - \dot{u}(x_2^\mathrm{r}, t)\right] \tag{4}$$

which should fulfill the condition $(1)_9$.

Note, that it was assumed that the first body is on the right and therefore its contact interface forms the left boundary point, x_1^ℓ. Analogously for the second body. For the one-bar contact Γ_c reduces to single-element set $\Gamma_\mathrm{c} = \{x_1^\ell\}$. All three sets Γ_u, Γ_σ, and Γ_c disjointly cover the boundaries of intervals $\boldsymbol{I}_i$.

2.3. Weak form of contact-impact problem via bi-penalty method

In this section, we introduce the weak form of the contact-impact problems via the bi-penalty method, for details see [25]. The Lagrangian functional, $\mathcal{L}(u, \dot{u})$ of the problem of interest corresponding to Eq. (1) is given as

$$\mathcal{L}(u, \dot{u}) = \mathcal{T}(\dot{u}) - (\mathcal{U}(u) - \mathcal{W}(u)) + \mathcal{W}_c(u, \dot{u}), \tag{5}$$

where

$$\mathcal{T}(\dot{u}) = \int_{\boldsymbol{I}} \frac{1}{2}\rho A \dot{u}^2 \,\mathrm{d}x \tag{6}$$

$$\mathcal{U}(u) = \int_{\boldsymbol{I}} \frac{1}{2} E A u'^2 \,\mathrm{d}x \tag{7}$$

$$\mathcal{W}(u) = \int_{\boldsymbol{I}} ubA \,\mathrm{d}x + \sum_{x\in\Gamma_\sigma} uA\bar{\sigma} \tag{8}$$

are the kinetic energy, the strain energy, and the work of external forces, respectively. Note, that the cross-section area is marked by A.

Bi-penalty method adds the penalization term to the (strain) energy (7) to enforce the zero-gap on the contact boundary [7] and at the same time, an extra term to the (kinetic) energy (6) to enforce the zero-velocity-gap on the contact boundary. This way, we define a penalization term associated to the contact interface as

$$\mathcal{W}_{\mathrm{c}}(u, \dot{u}) = -\frac{1}{2}\epsilon_{\mathrm{s}} A \langle g \rangle^2 + \frac{1}{2}\epsilon_{\mathrm{m}} A \langle \dot{g} \rangle^2, \tag{9}$$

where the operator $\langle \bullet \rangle$ are the so-called Macaulay's brackets defined as $\langle \bullet \rangle = \frac{|\bullet|+\bullet}{2}$. The parameters ϵ_{s} [kg m^{-2} s^{-2}] and ϵ_{m} [kg m^{-2}] are the stiffness and mass penalty parameters, respectively.

The standard procedure for the stationary solution of (5), defined as $\delta \int_{\boldsymbol{T}} \mathcal{L}_{\mathrm{p}}(u, \dot{u}) \,\mathrm{d}t = 0$, gives us

$$\int_{\boldsymbol{I}} \delta u \rho \ddot{u} \,\mathrm{d}x + \int_{\boldsymbol{I}} \delta u' E A u' \,\mathrm{d}x + H(g) A \left[\delta g(\epsilon_{\mathrm{s}} g + \epsilon_{\mathrm{m}} \ddot{g})\right] = \int_{\boldsymbol{I}} \delta u A b \,\mathrm{d}x + \sum_{x\in\Gamma_\sigma} \delta u A \bar{\sigma} \tag{10}$$

which is the framework for the finite element discretized equation of motion including the contact constraints by the bi-penalty method. Note the identity $\langle g \rangle = gH(g)$, where $H(g)$ is the Heaviside step function which ensures that the penalization term is active only in the case of penetration.

It is known that the standard/classical (stiffness) penalty method is not consistent [7], because it allows non-zero penetration at the contact interface. On the other hand, the zero-gap velocity condition represents a geometric condition of velocities equality at the contact interface. This geometric condition is required by the true solution. It is often enforced using the so-called persistence condition [12], where the product of the normal traction component and the gap velocity is required to be equal to zero. Although the bipenalty method in the derivation penalizes the gap velocity through the term which can be interpreted as kinetic energy in (9), however, after the application of Hamilton's variational principle, one gets a residual term that contains the second time derivative of the gap functions. Geometric condition of velocity equality at the contact interface thus is imposed indirectly by penalizing the second time derivative, which ultimately leads to smaller oscillations of the gap function and its velocity – stabilization of contact problem.

3. Bi-penalty method in finite element method for contact-impact problems

In the finite element procedures [38] for elastodynamic problems with contact constraints, the equations of motion yield the following system of nonlinear ordinary differential equations

$$\mathbf{M}\ddot{\mathbf{u}} + \mathbf{K}\mathbf{u} = \mathbf{r}(t) - \mathbf{r}_{\mathrm{c}}(\mathbf{u}, \ddot{\mathbf{u}}) \tag{11}$$

where $\mathbf{M}$ is the mass matrix, $\mathbf{K}$ is the stiffness matrix, $\mathbf{u}$ and $\ddot{\mathbf{u}}$ are nodal displacements and accelerations, $\mathbf{r}$ is the vector of external loading with time dependency, $\mathbf{r}_{\mathrm{c}}$ is the vector of contact forces. For a detailed derivation of the discretized equation of motion eq. (11) for the finite element method with the bi-penalty method see the work [25].

The linear FEM is applied in the rest of the paper for one-dimensional problems. The fully integrated elemental stiffness is assumed as

$$\hat{\mathbf{K}} = \frac{EA}{h_e}\begin{bmatrix} 1 & -1 \\ -1 & 1 \end{bmatrix} \tag{12}$$

The averaged mass matrix $\hat{\mathbf{M}}$ as a linear combination of the consistent mass matrix

$$\hat{\mathbf{M}}_C = \frac{\rho h_e A}{6}\begin{bmatrix} 2 & 1 \\ 1 & 2 \end{bmatrix} \tag{13}$$

and the lumped mass matrix

$$\hat{\mathbf{M}}_L = \frac{\rho h_e A}{2}\begin{bmatrix} 1 & 0 \\ 0 & 1 \end{bmatrix} \tag{14}$$

is given as

$$\hat{\mathbf{M}} = (1-\gamma)\hat{\mathbf{M}}_C + \gamma\hat{\mathbf{M}}_L = \frac{\rho h_e A}{6}\begin{bmatrix} 2+\gamma & 1-\gamma \\ 1-\gamma & 2+\gamma \end{bmatrix}. \tag{15}$$

In the previous text, it was assumed that cross-section area A, Young's modulus E, and density ρ are constant. h_e is the length of the finite element. As it is known the lumped mass matrices are preferred in explicit finite element analysis, but in this paper, we study the effect of contact oscillations due to the choice of the mass matrix.

In the bi-penalty formulation [25], the global contact residual vector, $\mathbf{r}_{\mathrm{c}}$, is assembled from the local counterparts $\hat{\mathbf{r}}_{\mathrm{c}}$ as the contribution of stiffness and mass terms to the contact residual vector which can be written as

$$\hat{\mathbf{r}}_{\mathrm{c}}(\hat{\mathbf{u}}, \ddot{\hat{\mathbf{u}}}) = \hat{\mathbf{M}}_{\mathrm{p}}\ddot{\hat{\mathbf{u}}} + \hat{\mathbf{K}}_{\mathrm{p}}\hat{\mathbf{u}} + \hat{\mathbf{f}}_{\mathrm{p}} \tag{16}$$

where

$$\hat{\mathbf{M}}_{\mathrm{p}} = \int_{\Gamma_{\mathrm{c}}} \epsilon_{\mathrm{m}} H(g)\mathbf{Z}\mathbf{Z}^{\mathrm{T}}\,\mathrm{d}S \qquad \hat{\mathbf{K}}_{\mathrm{p}} = \int_{\Gamma_{\mathrm{c}}} \epsilon_{\mathrm{s}} H(g)\mathbf{Z}\mathbf{Z}^{\mathrm{T}}\,\mathrm{d}S \qquad \hat{\mathbf{f}}_{\mathrm{p}} = \int_{\Gamma_{\mathrm{c}}} \epsilon_{\mathrm{s}} H(g)\mathbf{Z}g_0\,\mathrm{d}S \tag{17}$$

Here, $\hat{\mathbf{M}}_{\mathrm{p}}$ is the additional (penalized) elemental mass matrix due to inertia penalty, $\hat{\mathbf{K}}_{\mathrm{p}}$ is the additional (penalized) elemental stiffness matrix due to stiffness penalty, and $\hat{\mathbf{f}}_{\mathrm{p}}$ is the part of the elemental contact

force due to the initial gap g_0; g is the gap function; $H(g)$ is the Heaviside step function for prescribing active or inactive contact constraints; ϵ_{m} and ϵ_{s} are mass and stiffness penalty parameters; Γ_{c} is one of the contact surfaces, usually called slave, on which the contact terms are evaluated; the matrix $\mathbf{Z}$ represents an operator from the displacement field $\mathbf{u}$ to the gap function g in the contact

$$g = \mathbf{Z}^{\mathrm{T}}\mathbf{u} + g_0 \tag{18}$$

Remark. *Note that the gap function g is positive in separation and the Heaviside function $H(g)$ is one for $g > 0$. This means that the penalty matrices are acting only during separation. This is solved by defining $g \geq 0$ as the penetration.*

The particular form of matrix $\mathbf{Z}$ follows from the considered contact discretization. A comprehensive overview can be found e.g., in the textbook [7]. For the 1D case, see the definition of the gap function in (4), the corresponding representation of the gap function g takes the form

$$g = \mathbf{Z}^{\mathrm{T}}\mathbf{u} + g_0 = \begin{bmatrix} 1 & -1 \end{bmatrix} \begin{bmatrix} u_l \\ r_r \end{bmatrix} + g_0 \tag{19}$$

as well as for the Signorini problem (3)

$$g = \mathbf{Z}^{\mathrm{T}}\mathbf{u} + g_0 = \begin{bmatrix} 1 \end{bmatrix} \begin{bmatrix} u_l \end{bmatrix} + g_0 \tag{20}$$

where u_l and u_r are the displacements of the contacted nodes in the contact pair.

For the particular case of two bodies in contact, integration of (17) results in the following additional stiffness and mass matrices

$$\hat{\mathbf{K}}_{\mathrm{p}} = H(g)\frac{\beta_{\mathrm{s}} EA}{h_e}\begin{bmatrix} 1 & -1 \\ -1 & 1 \end{bmatrix}, \qquad \hat{\mathbf{M}}_{\mathrm{p}} = H(g)\frac{\beta_{\mathrm{m}}\rho h_e A}{2}\begin{bmatrix} 1 & -1 \\ -1 & 1 \end{bmatrix} \tag{21}$$

and for the Signorini problem

$$\hat{\mathbf{K}}_{\mathrm{p}} = H(g)\frac{\beta_{\mathrm{s}} EA}{h_e}\begin{bmatrix} 1 \end{bmatrix}, \qquad \hat{\mathbf{M}}_{\mathrm{p}} = H(g)\beta_{\mathrm{m}}\rho h_e A\begin{bmatrix} 1 \end{bmatrix}. \tag{22}$$

Here we have defined dimensionless stiffness and mass penalty parameters for the one-dimensional case as β_{m} and β_{s}, as follows

$$\beta_{\mathrm{s}} = \frac{h_e}{EA}\epsilon_{\mathrm{s}}, \quad \beta_{\mathrm{m}} = \frac{2}{\rho h_e A}\epsilon_{\mathrm{m}} \tag{23}$$

and their dimensionless penalty ratio

$$r = \frac{1+2\gamma}{6}\frac{\beta_s}{\beta_m}. \tag{24}$$

In the following, the necessary condition for the parameter r will be shown so that the stability limit for several types of mass matrix is not affected.

Remark. *The penalized mass matrix $\hat{\mathbf{M}}_{\mathrm{p}}$ is singular and the corresponding total mass included in this mass matrix is zero. This is very a good physical behavior of $\hat{\mathbf{M}}_{\mathrm{p}}$.*

4. Explicit time integration schemes for contact-impact problems

We now consider the time integration of the semi-discretized system (11) respecting the bi-penalty terms (16) in the framework of the central difference method in time [38] as

$$(\mathbf{M}^t + \mathbf{M}_{\mathrm{p}}^t)\frac{\mathbf{u}^{t+\Delta t} - 2\mathbf{u}^t + \mathbf{u}^{t-\Delta t}}{\Delta t^2} + (\mathbf{K}^t + \mathbf{K}_{\mathrm{p}}^t)\mathbf{u}^t - \mathbf{f}_{\mathrm{p}}^t - \mathbf{r}^t = \mathbf{0}. \tag{25}$$

Assuming that displacements are known at times $t - \Delta t$ and t, one can resolve unknown displacements at time $t + \Delta t$, where Δt denotes the time step size. Note, that the matrices $\mathbf{M}_{\mathrm{p}}^t$ and $\mathbf{K}_{\mathrm{p}}^t$ are time-dependent because they are associated with active contact constraints. In the following text, we mention the stability behaviour of the bi-penalized system and explicit time integration of the equation (25).

4.1. Stability limit of the bi-penalty method

It is known that the standard penalty method [1], where an additional stiffness term corresponding to contact boundary conditions is applied, significantly attacks the stability limit (the critical time step size Δt_{cr}) of the finite element model. Note, the stability limit for explicit time integration by the central difference method [40] is given as $\Delta t_{cr} = 2/\omega_{max}$, where ω_{max} is the maximum eigenfrequency of the discretized model.

For the averaged mass matrix with arbitrary γ, the maximum eigen-frequency of the separated finite element is given as

$$\omega_{max} = \sqrt{\frac{12}{1+2\gamma}}\frac{c_0}{h_e}, \tag{26}$$

therefore the stability limit is computed as

$$\Delta t_{cr} = 2/\omega_{max} = \sqrt{\frac{1+2\gamma}{3}}\frac{h_e}{c_0}. \tag{27}$$

where $c_0 = \sqrt{E/\rho}$ is the wave speed in a bar and h_e is the length of finite element.

The Courant number, let's define as

$$C = \frac{\Delta t}{\Delta t_{cr}} \tag{28}$$

where Δt is the time step size using in wave propagation simulations and thus $\Delta t = C\Delta t_{cr}$.

Generally, the critical time step size Δt_{cr} rapidly decreases with increasing penalty stiffness [1]. On the other hand, this numerical effect can be eliminated by a particular choice of additional mass penalty term [24]. The stability limit for the bi-penalty method has been studied in work of Kopačka [25], where the optimal ratio of stiffness and mass penalty parameters as $r = 1$ were found for one-dimensional problems with the lumped mass matrix. The general problem with respect to the stability of bi-penalized terms has been studied in the work of Hetherington [28]. The critical time step size Δt_{cr} associated with contact-free bodies are preserved for this optimal setting of mass penalty parameter with respect to the stiffness penalty parameter. Thus stability limit for the contact problem is not attacked by the stiffness penalty term. In

principle, one can integrate contact-impact problems by an arbitrary stable time step size $\Delta t < \Delta t_{cr}$. In Figs. 3, one can see the stability graphs for the Signorini and two element contact symmetric problems, where the dimensionless critical Courant number C_r is computed as $C_r = c_0 \Delta t_{cr}/h_e$ for the lumped mass matrix. For details of the stability analysis see work [25], where numerical tests have verified this stability analysis for the central difference method for direct time integration.

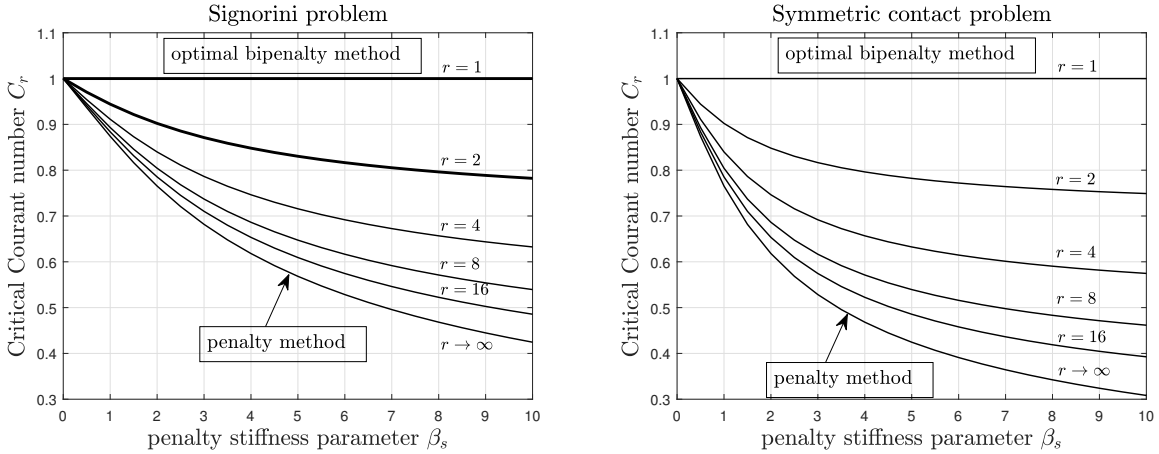

Figure 3: Stability limits for the bi-penalty method for the bi-penalized Signorini problem (on the left) and the symmetric contact problem (on the right): Dependence of the critical Courant number C_{r} on the dimensionless stiffness penalty β_{s} for selected dimensionless penalty ratios r with the lumped mass matrix. For details see work [25].

4.2. Optimal setting of the penalized mass matrix

From a general point of view, mass and stiffness penalty matrices present the same structure, see Eq. (17), where only the constants ε_m and ε_s are different. This means that there exists a linear relationship between $\hat{\mathbf{M}}_{\mathrm{p}}$ and $\hat{\mathbf{K}}_{\mathrm{p}}$. Let us then analyze the frequency content of the mass penalty matrix expressed in the form

$$\hat{\mathbf{M}}_{\mathrm{p}} = \alpha \hat{\mathbf{K}}_{\mathrm{p}} \tag{29}$$

where α is a free parameter $[1/s^2]$. Now, Let us find an "optimal" value of the parameter α, see [28] so that the maximum eigen-frequency of the penalized dynamic system ω_{max} defined as

$$[-\omega_{max}^2(\mathbf{M} + \mathbf{M}_{\mathrm{p}}) + (\mathbf{K} + \mathbf{K}_{\mathrm{p}})]\mathbf{\Phi}_{max} = \mathbf{0} \tag{30}$$

has the same maximum eigen-frequency ω_{max} and corresponding mode shape $\mathbf{\Phi}_{max}$ as the contact-free dynamic system expressed as

$$[-\omega_{max}^2\mathbf{M} + \mathbf{K}]\mathbf{\Phi}_{max} = \mathbf{0}. \tag{31}$$

We assume that ω_{max} is nonzero and the previous relationships need to satisfy the following relationship

$$\hat{\mathbf{M}}_{\mathrm{p}} = \frac{1}{\omega_{max}^2}\hat{\mathbf{K}}_{\mathrm{p}} \tag{32}$$

thus $\alpha = 1/\omega_{max}^2$, which is in an agreement with [28]. This is a very simple formula that can be used for the evaluation of the mass penalized matrix with arbitrary stiffness penalty parameters. Based on comparison of (21), (24), (26) and (32), the optimal setting of dimensionless penalty ratio is found to be $r = 1$.

It is needed to mention that ω_{max} is the maximum eigen-frequency of the finite element mesh in contact and it will be computed from

$$(-\omega^2\hat{\mathbf{M}} + \hat{\mathbf{K}})\hat{\mathbf{\Phi}} = \mathbf{0} \tag{33}$$

and ω_{max} for the 1D case studied in this paper is given by (26). It means that there is a strong coupling of the dynamic behaviour of finite elements in contact constraints and dynamic behaviour of the bi-penalty terms corresponding to contact constraints. The coupling of dynamics of contacted bodies and bi-penalty contact terms is through the maximum eigen-frequency ω_{max} of the finite elements in the contact constraints. The condition shown in (32) is a sufficient condition for the keeping of the same stability limit of a contact-free problem and bi-penalized contact problem. For that reason, one can estimate the stable time step size of contact-impact problems without a knowledge of contact constraints of bodies where the condition for penalized matrices (32) is valid. This evaluation of penalized stiffness and mass matrices for the bi-penalty method is given on elemental level, and the global matrices are assembled in a standard finite element process.

4.3. Central difference scheme for contact-impact problems

In this paper, we use the following form of the central difference (CD) scheme for explicit direct time integration of elastodynamic problems with contact constraints based on the bi-penalty method with the flowchart [38] as:

- Given $\mathbf{u}^t$, $\dot{\mathbf{u}}^{t-\Delta t/2}$ satisfying Dirichlet boundary conditions, and computed external force $\mathbf{r}^t$
- Contact search for given $\mathbf{u}^t$, compute gap vector $\mathbf{g}$ and contact forces $\mathbf{f}_{\mathrm{p}}^t = -\mathbf{K}_{\mathrm{p}}^t\mathbf{u}^t - \mathbf{f}_{\mathrm{p}}^0$
- Compute accelerations $\ddot{\mathbf{u}}^t = (\mathbf{M}^t + \mathbf{M}_{\mathrm{p}}^t)^{-1}(\mathbf{r}^t - \mathbf{K}^t\mathbf{u}^t + \mathbf{f}_{\mathrm{p}}^t)$
- Mid-point velocities $\dot{\mathbf{u}}^{t+\Delta t/2} = \dot{\mathbf{u}}^{t-\Delta t/2} + \Delta t\ddot{\mathbf{u}}^t$
- New displacements $\mathbf{u}^{t+\Delta t} = \mathbf{u}^t + \Delta t\dot{\mathbf{u}}^{t+\Delta t/2}$
- $t \to t + \Delta t$

Here, we used the lumped version of the mass matrix $\mathbf{M}$ by the row-summing. In general, the bi-penalized mass matrix $\mathbf{M}_{\mathrm{p}}^t$ is a symmetrical block diagonal matrix with terms corresponding to nodes in contacts, thus the inversion of total mass $(\mathbf{M}^t + \mathbf{M}_{\mathrm{p}}^t)^{-1}$ is a trivial numerical issue. For an efficient implementation of this approach, the partitioned analysis of the contact-impact problems via the localized Lagrangian multipliers [3] can be adopted.

4.4. Stabilized explicit predictor-corrector scheme for contact-impact problems

In the works [37], characteristics of the fully explicit time integration scheme with a stabilized technique for contact-impact problems were analyzed. For the predictor-corrector time scheme [41], it is needed to split the accelerations corresponding to the external/internal forces and accelerations corresponding to the contact forces as mentioned in [7]. After that, the time integration of each acceleration field is integrated in time separately. In essence, it is a predictor-corrector form for accelerations of corresponding external/internal forces and contact forces as, see [7],

$$\ddot{\mathbf{u}} = \ddot{\mathbf{u}}_{pred\,(bulk)} + \ddot{\mathbf{u}}_{corr\,(contact)} \tag{34}$$

where the predictor acceleration vector $\ddot{\mathbf{u}}_{pred}$ corresponds to external/internal forces $(\mathbf{r}^t - \mathbf{K}\mathbf{u}^t)$ and the corrector acceleration vector $\ddot{\mathbf{u}}_{pred}$ corresponds to the contact forces $\mathbf{r}_{\mathrm{c}}^t$.

The mentioned time integration scheme takes the following flowchart with splitting of bulk (contact-free problem) $\ddot{\mathbf{u}}_{pred}$ and contact accelerations $\ddot{\mathbf{u}}_{corr}^t$:

- Given $\mathbf{u}^t$, $\dot{\mathbf{u}}^{t-\Delta t/2}$, $\mathbf{r}^t$
- Compute accelerations of predictor phase $\ddot{\mathbf{u}}_{pred}^t = \mathbf{M}^{-1}(\mathbf{r}^t - \mathbf{K}\mathbf{u}^t)$
- Mid-point velocities of predictor phase $\dot{\mathbf{u}}_{pred}^{t+\Delta t/2} = \dot{\mathbf{u}}^{t-\Delta t/2} + \Delta t \ddot{\mathbf{u}}_{pred}^t$
- Displacements of predictor phase $\mathbf{u}_{pred}^{t+\Delta t} = \mathbf{u}^t + \Delta t \dot{\mathbf{u}}_{pred}^{t+\Delta t/2}$
- Contact search for given $\mathbf{u}_{pred}^{t+\Delta t}$, compute gap vector $\mathbf{g}$ and contact forces $\mathbf{f}_{\mathrm{p}\,pred} = -\mathbf{K}_{\mathrm{p}}\mathbf{u}_{pred}^{t+\Delta t} - \mathbf{f}_{\mathrm{p}}^0$
- Compute accelerations of corrector phase $\ddot{\mathbf{u}}_{corr}^t = (\mathbf{M} + \mathbf{M}_{\mathrm{p}})^{-1}(\mathbf{f}_{\mathrm{p}\,pred})$
- Compute total accelerations $\ddot{\mathbf{u}}^t = \ddot{\mathbf{u}}_{pred}^t + \ddot{\mathbf{u}}_{corr}^t$
- Mid-point velocities of corrector phase $\dot{\mathbf{u}}^{t+\Delta t/2} = \dot{\mathbf{u}}_{pred}^{t+\Delta t/2} + \Delta t \ddot{\mathbf{u}}_{corr}^t$
- New displacements of corrector phase $\mathbf{u}^{t+\Delta t} = \mathbf{u}^t + \Delta t \dot{\mathbf{u}}^{t+\Delta t/2}$
- Contact search for given $\mathbf{u}^{t+\Delta t}$, compute gap vector $\mathbf{g}$ and contact forces $\mathbf{f}_{\mathrm{p}}^{t+\Delta t} = -\mathbf{K}_{\mathrm{p}}\mathbf{u}^{t+\Delta t} - \mathbf{M}_{\mathrm{p}}\ddot{\mathbf{u}}^{t+\Delta t} - \mathbf{f}_{\mathrm{p}}^0$
- $t \to t + \Delta t$

In this two-time step scheme, bulk accelerations in the predictor phase $\ddot{\mathbf{u}}_{pred}^t$ are computed due to internal and external forces as a contact-free problem. It is calculated with the standard mass matrix $\mathbf{M}$. After updating of velocities and displacements, contact constraints are analyzed and contact forces $\mathbf{f}_{\mathrm{p}\,pred}$ are evaluated. For these contact forces, contact accelerations in the corrector phase $\ddot{\mathbf{u}}_{corr}^t$ are computed with the additional penalized mass matrix together with the mass matrix ($\mathbf{M}$+$\mathbf{M}_{\mathrm{p}}$) which needs inversion of this total mass matrix. After, the velocities and displacements are updated concerning these corrected accelerations taking into account contact constraints. Finally, the contact forces are evaluated in the consistent way, see the Asano's paper [26].

Remark. *In the corrector phase, the contact nodal forces* $\mathbf{f}_{\mathrm{p}\,pred}$ *correspond to the nodes in the contact; thus, the force vector is sparse. For that reason, the mass matrix* $\mathbf{M}+\mathbf{M}_{\mathrm{p}}$ *can be evaluated only for nodes in the contact and inverse of the total mass matrix* $(\mathbf{M}+\mathbf{M}_{\mathrm{p}})^{-1}$ *can be computed easily, because the matrix is blocked diagonal and the dimension of this matrix is small.*

Remark. *It can also be used a diagonalized version of the penalized mass matrix* $\mathbf{M}_{\mathrm{p}}$ *composed as a row-summing of absolute values and the inversion of* $(\mathbf{M}+\mathbf{M}_{p})^{-1}$ *becomes a trivial operation. In this case, the extra penalty masses are added only into the contact interfaces and the total mass is not preserved like in the consistent definition of the penalty mass matrix given by the definition (17).*

It is well known that the central difference method in time and linear finite element in space with the lumped mass matrix is a good choice of temporal-spatial discretization due to dispersion behaviour [42]. If one uses the time step size as a stability limit for regular mesh, the dispersion errors are eliminated and we are able to obtain an exact solution of elastic wave propagation in the bar. On the other hand, when we integrate using a time step size smaller than the stability limit, we obtain the stress distribution with stress spurious oscillations which are an outcome of the temporal-spatial discretizations.

4.5. Stabilized Park time integration scheme for contact-impact problems

For the correct solution of the impact contact problem, it is also needed to eliminate the stress spurious oscillations. An example of the time scheme, which is to able be to eliminate these numerical errors, is the Park time scheme [39]. This scheme is based on front-shock and pullback integration, where the wave speed is preserved and the numerical dispersion errors can be eliminated [43]. The time scheme has been presented in the work of Park [39] for the 1D case, and for multi-dimensional cases for separate integration of longitudinal and shear waves see [44, 42, 45]. Next, we plan to extend the Park time integration scheme to contact-impact problems in predictor-corrector explicit time sense for elimination stress wave propagation inside the elastic bars and contact forces at the same time.

The algorithm adopted for linear wave propagation problems uses the following steps:

- Given $\mathbf{u}^t, \dot{\mathbf{u}}^t, \ddot{\mathbf{u}}^t, \mathbf{r}^t$
- Front-shock displacement $\mathbf{u}_{fs}^{t+\Delta t_c} = \mathbf{u}^t + \Delta t_c \dot{\mathbf{u}}^t + \frac{\Delta t_c^2}{2}\ddot{\mathbf{u}}^t$ for given Δt_c
- Front-shock acceleration $\ddot{\mathbf{u}}_{fs}^{t+\Delta t_c} = \mathbf{M}^{-1}[\mathbf{r}^{t+\Delta t_c} - \mathbf{K}\mathbf{u}_{fs}^{t+\Delta t_c}]$
- Pullback interpolation $\mathbf{u}_{fs}^{t+\Delta t} = \mathbf{u}^t + \Delta t\dot{\mathbf{u}}^t + {\Delta t_c}^2\beta_1(\alpha)\ddot{\mathbf{u}}^t + {\Delta t_c}^2\beta_2(\alpha)\ddot{\mathbf{u}}_{fs}^{t+\Delta t_c}$ with $\alpha = \frac{\Delta t}{\Delta t_c}$, $\quad \beta_1(\alpha) = \frac{1}{6}\alpha\big(1+3\alpha-\alpha^2\big), \quad \beta_2(\alpha) = \frac{1}{6}\alpha\big(\alpha^2-1\big)$
- Pushforward displacement $\mathbf{u}_{cd}^{t+\Delta t} = \mathbf{u}^t + \Delta t\dot{\mathbf{u}}^t + \frac{\Delta t^2}{2}\ddot{\mathbf{u}}^t$
- Averaged displacement as predictor phase $\mathbf{u}_{pred}^{t+\Delta t} = \theta\mathbf{u}_{fs}^{t+\Delta t} + (1-\theta)\mathbf{u}_{cd}^{t+\Delta t}$ for given θ
- Acceleration for predictor phase $\ddot{\mathbf{u}}_{pred}^{t+\Delta t} = \mathbf{M}^{-1}\left[\mathbf{r}^{t+\Delta t} - \mathbf{K}\mathbf{u}_{pred}^{t+\Delta t}\right]$
- Velocity for predictor phase $\dot{\mathbf{u}}_{pred}^{t+\Delta t} = \dot{\mathbf{u}}^t + \frac{\Delta t}{2}\left(\ddot{\mathbf{u}}^t + \ddot{\mathbf{u}}_{pred}^{t+\Delta t}\right)$
- Contact search for given $\mathbf{u}_{pred}^{t+\Delta t}$, compute gap vector $\mathbf{g}$ and contact forces $\mathbf{f}_{\mathrm{p}\,pred} = -\mathbf{K}_{\mathrm{p}}\mathbf{u}_{pred}^{t+\Delta t} - \mathbf{f}_{\mathrm{p}}^0$

- Compute accelerations of corrector phase $\ddot{\mathbf{u}}_{corr}^{t+\Delta t} = (\mathbf{M} + \mathbf{M}_{\mathrm{p}})^{-1}(\mathbf{f}_{\mathrm{p}\,pred})$
- Compute total accelerations $\ddot{\mathbf{u}}^{t+\Delta t} = \ddot{\mathbf{u}}_{pred}^{t+\Delta t} + \ddot{\mathbf{u}}_{corr}^{t+\Delta t}$
- Compute total velocities $\dot{\mathbf{u}}^{t+\Delta} = \dot{\mathbf{u}}_{pred}^{t+\Delta t} + \frac{\Delta t}{2}\ddot{\mathbf{u}}_{corr}^{t+\Delta t}$
- Total displacement $\mathbf{u}^{t+\Delta t} = \mathbf{u}_{pred}^{t+\Delta t}$
- Search contact for given $\mathbf{u}^{t+\Delta t}$, compute gap vector $\mathbf{g}$ and contact forces $\mathbf{f}_{\mathrm{p}}^{t+\Delta t} = -\mathbf{K}_{\mathrm{p}}\mathbf{u}^{t+\Delta t} - \mathbf{M}_{\mathrm{p}}\ddot{\mathbf{u}}^{t+\Delta t} - \mathbf{f}_{\mathrm{p}}^{0}$
- $t \rightarrow t + \Delta t$

The stabilized *Park* time integration scheme can be characterized as the three-time step scheme with two steps for the wave propagation problem without including contact constraints, for details see [39]. The first step uses the critical time step size Δt_{cr} and the second one the complete time step size Δt which is smaller than Δt_{cr}. The last step includes the contact constraints into the response without producing spurious oscillations in the stress distribution along the bars. The scheme produces excellent results with the lumped mass matrix due to temporal-spatial dispersion errors in the numerical model. We choice the time step size as $\Delta t = 0.5\Delta t_{cr}$ and averaged parameter as $\theta = 0.5$ which is based on numerical tests in [39].

5. Numerical tests — impact of elastic bars

In this section, we present two tests for analysis of the behaviour of the suggested approach for finite element modelling of contact-impact problems — the Signorini (impact of a bar on a rigid wall) and Huněk problems (impact of two elastic bars).

5.1. Numerical test I — Signorini problem

In the first example, we study an one-dimensional impact problem of an elastic bar against a rigid wall. This one-dimensional test is well known as the Signorini problem.

5.1.1. Problem definition

A scheme of this test is depicted in Figure 4. The bar is moving to the right side with the constant velocity $v_{01} = 0.1\,[\mathrm{m/s}]$. The geometrical, material and numerical parameters were set up as: the length $L = 10\,[\mathrm{m}]$, the Young's modulus $E = 100\,[\mathrm{Pa}]$, the mass density $\rho = 0.01\,[\mathrm{kg \cdot m^{-3}}]$, the cross-sectional area $A = 1\,[\mathrm{m^2}]$. The initial contact gap is $g_0 = 0\,[\mathrm{m}]$ and the duration time is $T = 0.3\,[\mathrm{s}]$. The value of the contact force from the analytical prediction is $F_0 = A\rho c_0 v_0 = -0.1\,[\mathrm{N}]$ for $t = 0 \ldots 0.2\,[\mathrm{s}]$ and zero otherwise, see [46], where wave speed in a bar $c_0 = \sqrt{E/\rho} = 100\,[\mathrm{m/s}]$.

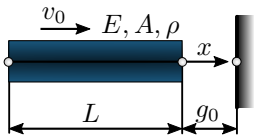

Figure 4: A scheme of one-dimensional impact problem of an elastic bar against a rigid wall - the Signorini problem.

5.1.2. Numerical parameters

For numerical verification of the methodology for this test, we set β_s as follows $\beta_s = \{1e0; 1e4; 1e8; 1.e12\}$ and β_m is set with respect to optimal value given by Eq. (24) with $r = 1$ or equivalently via (32). The number of finite linear elements for the bar, $n = 100$, thus the uniform finite element lengths are set up as $h_e = 0.1\,[\mathrm{m}]$.

The time step size is chosen as $\Delta t = C\Delta t_{cr}$, where Courant dimensionless number is used $C = 0.5$. The critical time step size is set with respect to (27) for given γ. This time step size is stable for all value of β_s with optimal setting of β_m. We present results of the contact-impact problem in the form of the time history of kinetic and strain energies and work of contact forces, the time history of dimensionless gap function g/h_e and the time history of contact force. Results for the consistent ($\gamma = 0$), averaged ($\gamma = 0.5$) and lumped ($\gamma = 1$) mass matrices are presented.

5.1.3. Results for CD method

In Fig. 5, one can see the results of the test obtained by the central difference method for the penalty stiffness parameter $\beta_s = 1e0$ and corresponding optimal β_m. All three type of mass matrices were taken into account. The histories of the contact forces show spurious oscillations. The consistent mass matrix produces a higher level of spurious oscillation which is given by spurious oscillations of stress during wave processes in the bar. This effect is not so evident for the lumped mass and averaged mass matrix due to better dispersion behaviour of FEM in wave propagation. The relative gap is $g/h_e = -1e-3$. For $\beta_s = 1e0$ the results are physically correct, where the penalty stiffness has the same of order as the stiffness of finite elements in the contact. One can also see that the contact energy comes to zero for $\beta_s = 1e0$.

In Fig. 6, the results for the CD scheme, $\beta_s = 1e4$ and the lumped mass matrix are presented. The results show a stable solution but the spurious oscillations of gap function and contact forces are observed. Based on numerical observation, there is a $zig-zag$ effect in contact constraint where contact is switched-on and switched-off. It is a product of a large value of penalty stiffness parameter. Naturally, one can see this behaviour for a large value of β_s independently of mass matrix type. The stress distributions in the bar for all three types of the mass matrix are depicted in Fig. 7. In contact, the oscillations of stress occur. This behaviour relating to spurious oscillations of contact forces was explained in [2] and it is an outcome of a one-time step scheme. Therefore, we employ in the next text the stabilized predictor-corrector scheme and

Park schemes, where the integration of bulk and contact accelerations are split.

5.1.4. Results for the stabilized predictor-corrector scheme

In Figs. 8, we present the results obtained by the the stabilized predictor-corrector scheme for $\beta_s = 1e4$. One can see the results of time histories of contact forces, gap functions and energy balance. The results are shown for all three mass matrix types. One can see superior results for the lumped mass matrix. Based on several tests for different values of $\beta_s = \{1e0, 1e4, 1e8, 1e12\}$, the results are not influenced of the choice of the stiffness penalty parameter β_s with condition of the optimal setting of β_m. The same results can be detected for the averaged mass matrix. On the other hand, the consistent mass matrix produces the spurious oscillations at the end of the time history of active contact force which is an outcome of spurious oscillations of stresses along the bar as a product of dispersion behaviour of FEM. This effect is depicted in Fig. 9 as stress distribution along the bar for all three types of the mass matrix. It is needed to mention that the stress oscillations on the contacted side were eliminated by using the stabilized predictor-corrector time scheme. We can speak about the stabilization effect of this time scheme on the stress and contact force results. The corresponding of the dimensionless gap values with respect to the β_s are $g/h_e = \{-1e-4, 1e-7, 1e-10, 1e-15\}$ for all three mass matrix type. The convergence properties of this predictor-corrector time scheme with the bi-penalty method is observed.

5.1.5. Results for Park method

The *Park* non-spurious time scheme with connection with the linear finite element and lumped mass matrix has been analyzed as a suitable approach for eliminating of stress spurious oscillations [39]. Therefore, we adopted this scheme in the predictor-corrector form for contact-impact problems. We have to mention that this scheme produces superior results of stress distributions for the lumped mass matrix and we apply only this mass matrix for the computations in this part.

In Fig.10, the results of the Park scheme with stabilization for contact-impact problems are presented for $\beta_s = 1e4$ with the optimal setting of β_m. The computation gives excellent results for a time history of contact forces. But only the oscillations can be seen at the initial time of contact activation. The same results are found for the different values of β_s and we could say that the results do not depend on β_s. In Fig. 11, the stress distribution along the bar is shown. One can see the distribution without dominant spurious oscillations inside the bar and also no spurious oscillations at the contact area. Based on that results, the Park scheme with predictor-corrector explicit time scheme can eliminate spurious oscillation effects of both, stress waves propagating along the bar, and contact forces.

5.2. Numerical test II — Impact of two bars with different lengths (Huněk problem)

In the second example, we study an one-dimensional contact-impact problem of two elastic bars with different lengths prescribed in the work of Huněk [47].

5.2.1. Problem definition

A scheme of this test is depicted in Figure 12. The left bar is moving to the right with the constant velocity $v_{01} = 0.1\,[\mathrm{m/s}]$. The right bar with fixed right-hand side is at the rest. The geometrical, material and numerical parameters were set up: the lengths $L_1 = 10\,[\mathrm{m}]$ and $L_2 = 20\,[\mathrm{m}]$, the Young's modulus $E_1 = E_2 = 100\,[\mathrm{Pa}]$, the mass density $\rho_1 = \rho_2 = 0.01\,[\mathrm{kg \cdot m^{-3}}]$, the cross-sectional area $A_1 = A_2 = 1\,[\mathrm{m^2}]$, the number of finite linear elements for each bar $n_1 = 50$, $n_2 = 100$, thus the finite element lengths are set up as $h_1 = h_2 = 0.2\,[\mathrm{m}]$, the initial contact gap $g_0 = 0\,[\mathrm{m}]$, the duration time $T = 0.7\,[\mathrm{s}]$. The value of the contact force from the analytical prediction is $F_0 = 0.05\,[\mathrm{N}]$ for $t = 0 \ldots 0.2\,[\mathrm{s}]$ and $t = 0.4 \ldots 0.6\,[\mathrm{s}]$ and zero otherwise, see [46].

5.2.2. Numerical parameters

In this test, we use the same definition of dimensionless stiffness and mass penalty parameters for the bi-penalty method as in the previous case with $r = 1$. The mass matrix is of the lumped type. The dimensionless stiffness penalty parameter was as follows: $\beta_s = \{1e0;\ 1e4;\ 1e8;\ 1e12\}$. The time step size was also the same as in the previous test.

5.2.3. Results

In Figure 13, one can see the time histories of contact forces between two elastic bars from Fig. 12 computed by the central difference method, the stabilized explicit predictor-corrector scheme and the Park scheme with stabilization of contact forces. The value of $\beta_s = 1e4$ was chosen, β_m was set with respect to the optimal stability limit as $r = 1$. For the CD method, the spurious oscillations occur as in the Signorini problems. Against, the solutions for the stabilized explicit predictor-corrector scheme and Park schemes. The stabilized predictor-corrector scheme gives the history of contact forces with the low level of spurious oscillations, which is an outcome of the stress spurious oscillation inside the bar. The Park scheme gives the more correct history of contact forces due to the elimination of stress spurious oscillations. One can observe the same character of the time history of contact forces for all three time-schemes for different values of β_s.

Conclusions

A numerical approach for one-dimensional contact-impact problems modelled by the finite element method has been presented. The approach is based on the combination of the bi-penalty stabilization method with time integration in a predictor-corrector form. Thanks to the bi-penalty method, we can retain the stability limit of contact-free problems. We also have found evidence of the optimal setting of the ratio of mass and stiffness penalty parameters for the bi-penalty term, that it depends on the maximum eigen-frequency of the finite element meshes in contact. In time-stepping, a modification of the explicit method with the splitting of bulk and contact accelerations has been used. In this case, we compare the

results of the central difference method, its stabilized predictor-corrector version and the Park scheme with predictor-corrector parts. Based on the results on numerical tests, one can see that the bi-penalty stabilization works, and the predictor-corrector form of the time stepping is needed for elimination of contact force oscillations.

Furthermore, we have proposed a method to eliminate spurious oscillations of contact forces in the impact of elastic bars. The Park scheme gives us more accurate solutions concerning stress spurious oscillations and contact forces, and it is preferred in the numerical modelling of contact-impact problems concerning contact forces and stress propagation.

Based on the numerical tests, we can conclude that a motivated approach is an efficient tool for accurate modelling of contact-impact problems with minimum pollution of contact force by spurious oscillations. The results obtained by the stabilized explicit schemes in the connection with the bi-penalty method are *less sensitive* to the choice of the penalty parameter in contrast to the standard penalty approach. The gap function during the contact state converges correctly to zero for higher values of the penalty stiffness parameter. This issue needs a mathematical proof as in future work.

As future work, we will focus on applications of the presented approach to multidimensional problems, analyzing its performance, stability and accuracy with more complicated geometries and higher-order spatial discretization [48]. An important task to solve in a correct way is contact-impact problems of heterogeneous bodies with different mesh sizes, where the stability limits for each contacted bodies are different.

Acknowledgment

The work of Radek Kolman and Ján Kopačka were supported by the grant projects with No. 19-04956S of the Czech Science Foundation (CSF) within institutional support RVO:61388998 and the Centre of Excellence for Nonlinear Dynamic Behaviour of Advanced Materials in Engineering CZ.02.1.01/0.0/0.0/15_003/0000493 (Excellent Research Teams) in the framework of Operational Programme Research, Development and Education. K. C. Park was partially supported by the contract (#G06200018) from the Korean Atomic Energy Research Institute to KAIST.

[1] T. Belytschko, M. O. Neal, Contact-impact by the pinball algorithm with penalty and lagrangian methods, International Journal for Numerical Methods in Engineering 31 (3) (1991) 547–572. doi:10.1002/nme.1620310309.
URL http://dx.doi.org/10.1002/nme.1620310309

[2] N. J. Carpenter, R. L. Taylor, M. G. Katona, Lagrange constraints for transient finite element surface contact, International Journal for Numerical Methods in Engineering 32 (1) (1991) 103–128. doi:10.1002/nme.1620320107.
URL http://dx.doi.org/10.1002/nme.1620320107

[3] J. A. González, K. C. Park, C. A. Felippa, Partitioned formulation of frictional contact problems using localized lagrange multipliers, Communications in Numerical Methods in Engineering 22 (4) (2006) 319–333. arXiv:https://onlinelibrary.wiley.com/doi/pdf/10.1002/cnm.821, doi:10.1002/cnm.821.
URL https://onlinelibrary.wiley.com/doi/abs/10.1002/cnm.821

[4] T. A. Laursen, V. Chawla, Design of energy conserving algorithms for frictionless dynamic contact problems, International Journal for Numerical Methods in Engineering 40 (5) (1997) 863–886. doi:10.1002/(SICI)1097-0207(19970315)40:5<863::AID-NME92>3.0.CO;2-V.
URL http://dx.doi.org/10.1002/(SICI)1097-0207(19970315)40:5<863::AID-NME92>3.0.CO;2-V

[5] Z. Dostál, T. Kozubek, M. Sadowska, V. Vondrák, Scalable Algorithms for Contact Problems, 1st Edition, Springer, 2017.

[6] B. Wohlmuth, Variationally consistent discretization schemes and numerical algorithms for contact problems, Acta Numerica 20 (2011) 569734. doi:10.1017/S0962492911000079.

[7] P. Wriggers, Computational contact mechanics, 2nd Edition, Springer, Berlin; New York, 2006.
URL http://www.scribd.com/doc/9326570/Computational-Contact-Mechanics

[8] T. J. Hughes, R. L. Taylor, J. L. Sackman, A. Curnier, W. Kanoknukulchai, A finite element method for a class of contact-impact problems, Computer Methods in Applied Mechanics and Engineering 8 (3) (1976) 249 – 276. doi:https://doi.org/10.1016/0045-7825(76)90018-9.
URL http://www.sciencedirect.com/science/article/pii/0045782576900189

[9] R. L. Taylor, P. Papadopoulos, On a finite element method for dynamic contact/impact problems, International Journal for Numerical Methods in Engineering 36 (12) (1993) 2123–2140. arXiv:https://onlinelibrary.wiley.com/doi/pdf/10.1002/nme.1620361211, doi:10.1002/nme.1620361211.
URL https://onlinelibrary.wiley.com/doi/abs/10.1002/nme.1620361211

[10] F. Armero, E. Petocz, Formulation and analysis of conserving algorithms for frictionless dynamic contact/impact problems, Computer Methods in Applied Mechanics and Engineering 158 (3–4) (1998) 269–300. doi:10.1016/S0045-7825(97)00256-9.
URL http://www.sciencedirect.com/science/article/pii/S0045782597002569

[11] F. Armero, E. Petcz, A new dissipative time-stepping algorithm for frictional contact problems: formulation and analysis, Computer Methods in Applied Mechanics and Engineering 179 (1) (1999) 151 – 178. doi:https://doi.org/10.1016/S0045-7825(99)00036-5.
URL http://www.sciencedirect.com/science/article/pii/S0045782599000365

[12] T. A. Laursen, G. R. Love, Improved implicit integrators for transient impact problemsgeometric admissibility within the conserving framework, International Journal for Numerical Methods in Engineering 53 (2) (2002) 245–274. arXiv:https://onlinelibrary.wiley.com/doi/pdf/10.1002/nme.264, doi:10.1002/nme.264.
URL https://onlinelibrary.wiley.com/doi/abs/10.1002/nme.264

[13] J. Hallquist, G. Goudreau, D. Benson, Sliding interfaces with contact-impact in large-scale lagrangian computations, Computer Methods in Applied Mechanics and Engineering 51 (1) (1985) 107 – 137. doi:https://doi.org/10.1016/0045-7825(85)90030-1.
URL http://www.sciencedirect.com/science/article/pii/0045782585900301

[14] D. J. Benson, J. O. Hallquist, A single surface contact algorithm for the post-buckling analysis of shell structures, Computer Methods in Applied Mechanics and Engineering 78 (2) (1990) 141 – 163. doi:https://doi.org/10.1016/0045-7825(90)90098-7.
URL http://www.sciencedirect.com/science/article/pii/0045782590900987

[15] D. J. Benson, Computational methods in lagrangian and eulerian hydrocodes, Computer Methods in Applied Mechanics and Engineering 99 (2) (1992) 235 – 394. doi:https://doi.org/10.1016/0045-7825(92)90042-I.
URL http://www.sciencedirect.com/science/article/pii/004578259290042I

[16] M. W. Heinstein, F. J. Mello, S. W. Attaway, T. A. Laursen, Contactimpact modeling in explicit transient dynamics, Computer Methods in Applied Mechanics and Engineering 187 (3) (2000) 621 – 640. doi:https://doi.org/10.1016/S0045-7825(99)00342-4.

URL http://www.sciencedirect.com/science/article/pii/S0045782599003424

[17] C. Kane, E. Repetto, M. Ortiz, J. Marsden, Finite element analysis of nonsmooth contact, Computer Methods in Applied Mechanics and Engineering 180 (1) (1999) 1 – 26. doi:https://doi.org/10.1016/S0045-7825(99)00034-1.
URL http://www.sciencedirect.com/science/article/pii/S0045782599000341

[18] F. Cirak, M. West, Decomposition contact response (dcr) for explicit finite element dynamics, International Journal for Numerical Methods in Engineering 64 (8) (2005) 1078–1110. arXiv:https://onlinelibrary.wiley.com/doi/pdf/10.1002/nme.1400, doi:10.1002/nme.1400.
URL https://onlinelibrary.wiley.com/doi/abs/10.1002/nme.1400

[19] P. Otto, L. De Lorenzis, J. F. Unger, A regularized model for impact in explicit dynamics applied to the split hopkinson pressure bar, Computational Mechanics 58 (4) (2016) 681–695. doi:10.1007/s00466-016-1311-1.
URL https://doi.org/10.1007/s00466-016-1311-1

[20] P. Otto, L. Lorenzis, J. F. Unger, Explicit dynamics in impact simulation using a nurbs contact interface, International Journal for Numerical Methods in Engineering n/a (n/a). arXiv:https://onlinelibrary.wiley.com/doi/pdf/10.1002/nme.6264, doi:10.1002/nme.6264.
URL https://onlinelibrary.wiley.com/doi/abs/10.1002/nme.6264

[21] C. A. Felippa, Error analysis of penalty function techniques for constraint definition in linear algebraic systems, International Journal for Numerical Methods in Engineering 11 (4) (1977) 709–728. arXiv:https://onlinelibrary.wiley.com/doi/pdf/10.1002/nme.1620110408, doi:10.1002/nme.1620110408.
URL https://onlinelibrary.wiley.com/doi/abs/10.1002/nme.1620110408

[22] C. A. Felippa, Iterative procedures for improving penalty function solutions of algebraic systems, International Journal for Numerical Methods in Engineering 12 (5) (1978) 821–836. arXiv:https://onlinelibrary.wiley.com/doi/pdf/10.1002/nme.1620120508, doi:10.1002/nme.1620120508.
URL https://onlinelibrary.wiley.com/doi/abs/10.1002/nme.1620120508

[23] H. M. de la Fuente, C. A. Felippa, Ephemeral penalty functions for contact-impact dynamics, Finite Elements in Analysis and Design 9 (3) (1991) 177 – 191. doi:https://doi.org/10.1016/0168-874X(91)90031-S.
URL http://www.sciencedirect.com/science/article/pii/0168874X9190031S

[24] J. Hetherington, A. Rodríguez-Ferran, H. Askes, The bipenalty method for arbitrary multipoint constraints, International Journal for Numerical Methods in Engineering 93 (5) (2013) 465–482. doi:10.1002/nme.4389.
URL http://dx.doi.org/10.1002/nme.4389

[25] J. Kopačka, A. Tkachuk, D. Gabriel, R. Kolman, M. Bischoff, J. Plešek, On stability and reflection-transmission analysis of the bipenalty method in contact-impact problems: A one-dimensional, homogeneous case study, International Journal for Numerical Methods in Engineering 113 (10) (2018) 1607–1629. arXiv:https://onlinelibrary.wiley.com/doi/pdf/10.1002/nme.5712, doi:10.1002/nme.5712.
URL https://onlinelibrary.wiley.com/doi/abs/10.1002/nme.5712

[26] N. Asano, A virtual work principle using penalty function method for impact contact problems of two bodies, Bulletin of JSME 29 (249) (1986) 731–736. doi:10.1299/jsme1958.29.731.

[27] J. Hetherington, H. Askes, Penalty methods for time domain computational dynamics based on positive and negative inertia, Computers & Structures 87 (23–24) (2009) 1474–1482. doi:10.1016/j.compstruc.2009.05.011.
URL http://www.sciencedirect.com/science/article/pii/S0045794909001692

[28] J. Hetherington, A. Rodríguez-Ferran, H. Askes, A new bipenalty formulation for ensuring time step stability in time domain computational dynamics, International Journal for Numerical Methods in Engineering 90 (3) (2012) 269–286. doi:10.1002/nme.3314.
URL http://dx.doi.org/10.1002/nme.3314

[29] K. C. Park, J. C. Chiou, Stabilization of computational procedures for constrained dynamical systems, Journal of Guidance, Control, and Dynamics 11 (4) (1988) 365 – 370. doi:doi:10.2514/3.20320.

[30] J. Baumgarte, Stabilization of constraints and integrals of motion in dynamical systems, Computer methods in applied mechanics and engineering 1 (1) (1972) 1–16.

[31] E. A. Paraskevopoulos, C. G. Panagiotopoulos, G. D. Manolis, Imposition of time-dependent boundary conditions in fem formulations for elastodynamics: critical assessment of penalty-type methods, Computational Mechanics 45 (2) (2009) 157. doi:10.1007/s00466-009-0428-x.
URL https://doi.org/10.1007/s00466-009-0428-x

[32] D. Doyen, A. Ern, S. Piperno, Time-Integration Schemes for the Finite Element Dynamic Signorini Problem, SIAM Journal on Scientific Computing 33 (1) (2011) 223–249. doi:10.1137/100791440.
URL http://epubs.siam.org/doi/abs/10.1137/100791440

[33] P. Deuflhard, R. Krause, S. Ertel, A contact-stabilized newmark method for dynamical contact problems, International Journal for Numerical Methods in Engineering 73 (9) (2008) 1274–1290. doi:10.1002/nme.2119.
URL http://dx.doi.org/10.1002/nme.2119

[34] H. B. Khenous, P. Laborde, Y. Renard, Mass redistribution method for finite element contact problems in elastodynamics, European Journal of Mechanics - A/Solids 27 (5) (2008) 918–932. doi:10.1016/j.euromechsol.2008.01.001.

[35] Y. Renard, The singular dynamic method for constrained second order hyperbolic equations: Application to dynamic contact problems, Journal of Computational and Applied Mathematics 234 (3) (2010) 906–923. doi:10.1016/j.cam.2010.01.058.
URL http://www.sciencedirect.com/science/article/pii/S0377042710000713

[36] A. Tkachuk, Variational methods for consistent singular and scaled mass matrices, Ph.D. thesis, Institut für Baustatik und Baudynamik der Universität Stuttgart, Stuttgart (2013).

[37] S. R. Wu, A variational principle for dynamic contact with large deformation, Computer Methods in Applied Mechanics and Engineering 198 (21) (2009) 2009 – 2015, advances in Simulation-Based Engineering Sciences Honoring J. Tinsley Oden. doi:https://doi.org/10.1016/j.cma.2008.12.013.
URL http://www.sciencedirect.com/science/article/pii/S0045782509000139

[38] T. Belytschko, W. K. Liu, B. Moran, Nonlinear finite elements for continua and structures, Wiley, Chichester, 2008.

[39] K. C. Park, S. J. Lim, H. Huh, A method for computation of discontinuous wave propagation in heterogeneous solids: basic algorithm description and application to one-dimensional problems, International Journal for Numerical Methods in Engineering 91 (6) (2012) 622–643. arXiv:https://onlinelibrary.wiley.com/doi/pdf/10.1002/nme.4285, doi:10.1002/nme.4285.
URL https://onlinelibrary.wiley.com/doi/abs/10.1002/nme.4285

[40] K. C. Park, Practical aspects of numerical time integration, Computers & Structures 7 (3) (1977) 343 – 353. doi:https://doi.org/10.1016/0045-7949(77)90072-4.
URL http://www.sciencedirect.com/science/article/pii/0045794977900724

[41] T. J. R. Hughes, The finite element method: linear static and dynamic finite element analysis, Dover Publications, Mineola, NY, 2000.

[42] R. Kolman, S. S. Cho, K. C. Park, Efficient implementation of an explicit partitioned shear and longitudinal wave propagation algorithm, International Journal for Numerical Methods in Engineering 107 (7) (2016) 543–579. arXiv:https://onlinelibrary.wiley.com/doi/pdf/10.1002/nme.5174, doi:10.1002/nme.5174.
URL https://onlinelibrary.wiley.com/doi/abs/10.1002/nme.5174

[43] R. Kolman, J. Plešek, J. Červ, M. Okrouhlík, P. Pařík, Temporal-spatial dispersion and stability analysis of finite element method in explicit elastodynamics, International Journal for Numerical Methods in Engineering 106 (2) (2016) 113–128.

arXiv:https://onlinelibrary.wiley.com/doi/pdf/10.1002/nme.5010, doi:10.1002/nme.5010.
URL https://onlinelibrary.wiley.com/doi/abs/10.1002/nme.5010

[44] S. S. Cho, K. C. Park, H. Huh, A method for multidimensional wave propagation analysis via component-wise partition of longitudinal and shear waves, International Journal for Numerical Methods in Engineering 95 (3) (2013) 212–237. arXiv:https://onlinelibrary.wiley.com/doi/pdf/10.1002/nme.4495, doi:10.1002/nme.4495.
URL https://onlinelibrary.wiley.com/doi/abs/10.1002/nme.4495

[45] S. S. Cho, R. Kolman, J. A. Gonzlez, K. C. Park, Explicit multistep time integration for discontinuous elastic stress wave propagation in heterogeneous solids, International Journal for Numerical Methods in Engineering 118 (5) (2019) 276–302. arXiv:https://onlinelibrary.wiley.com/doi/pdf/10.1002/nme.6027, doi:10.1002/nme.6027.
URL https://onlinelibrary.wiley.com/doi/abs/10.1002/nme.6027

[46] K. F. Graff, Wave Motion in Elastic Solids, Clarendon Press, 1975.

[47] I. Huněk, On a penalty formulation for contact-impact problems, Computers & Structures 48 (2) (1993) 193 – 203. doi:http://dx.doi.org/10.1016/0045-7949(93)90412-7.
URL http://www.sciencedirect.com/science/article/pii/0045794993904127

[48] R. Kolman, M. Okrouhlík, A. Berezovski, D. Gabriel, J. Kopačka, J. Plešek, B-spline based finite element method in one-dimensional discontinuous elastic wave propagation, Applied Mathematical Modelling 46 (2017) 382 – 395. doi:https://doi.org/10.1016/j.apm.2017.01.077.
URL http://www.sciencedirect.com/science/article/pii/S0307904X17300835

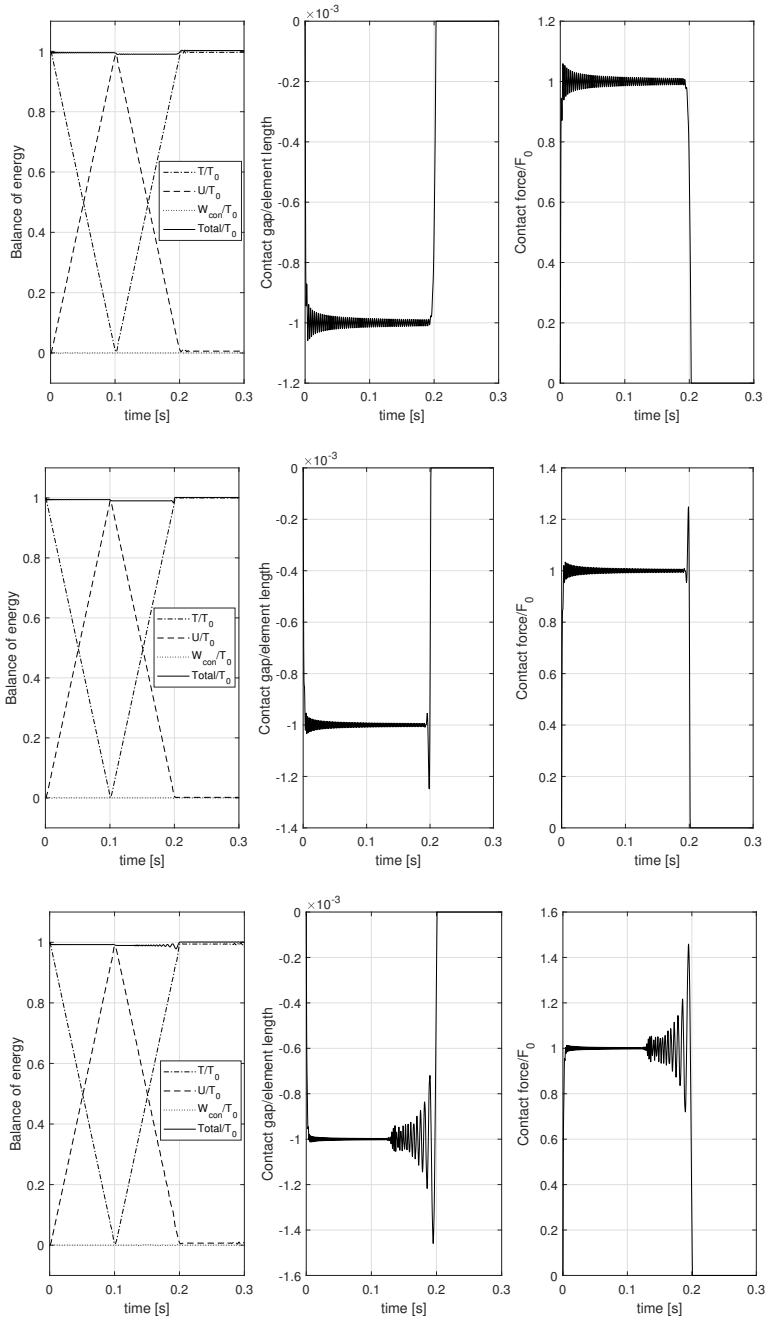

Figure 5: Results of the Signorini problem obtained by the central difference method with $C = 0.5$, $\beta_s = 1e0$, optimal setting of β_m, for lumped (above), averaged (middle) and consistent (below) mass matrix: Balance of energy in time (on the left), the time history of gap function (in the middle), the time history of contact force (on the right).

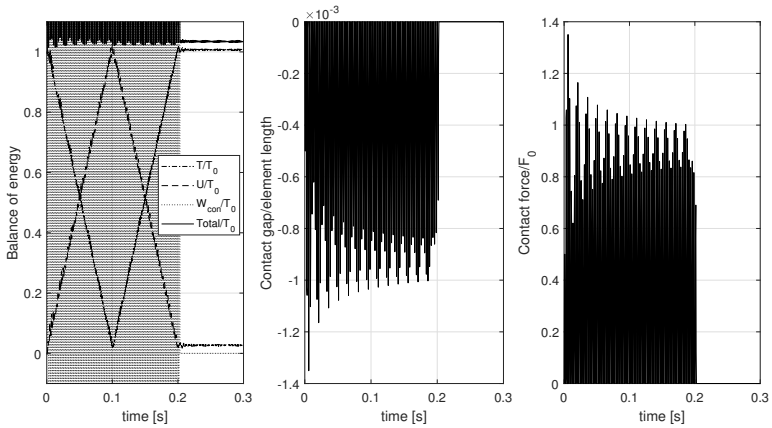

Figure 6: Results of the Signorini problem obtained by the central difference method with $C = 0.5$, $\beta_s = 1e4$, optimal setting of β_m, for lumped mass matrix: Balance of energy in time (on the left), the time history of gap function (in the middle), the time history of contact force (on the right) .

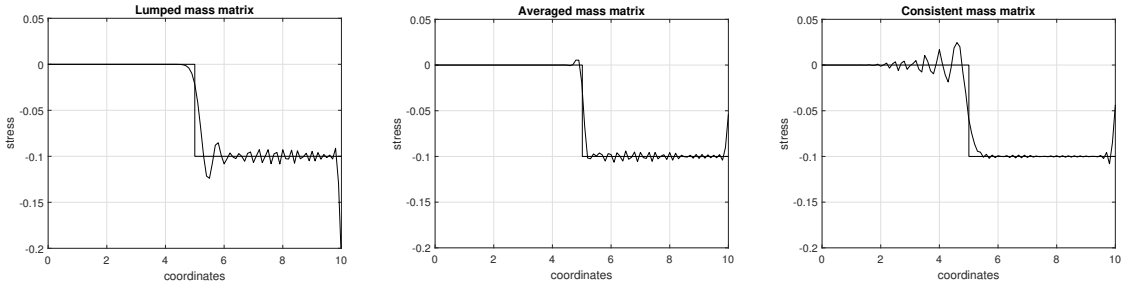

Figure 7: Stress distributions at the time $t = 0.5$ $[s]$ as results of the Signorini problem obtained by the central difference method with $C = 0.5$, $\beta_s = 1e4$, optimal setting of β_m, lumped (left), averaged (middle) and consistent (right) mass matrices. The analytical solution of wave propagation is attached.

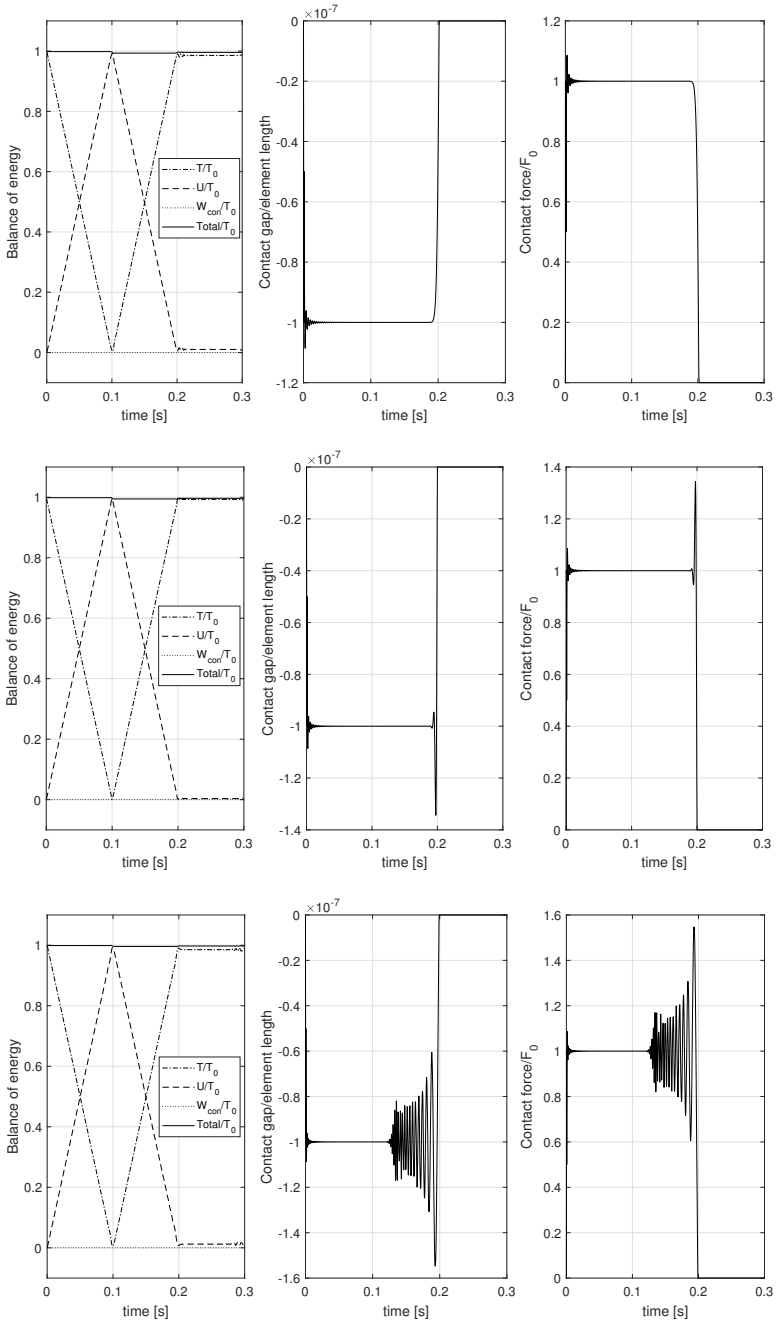

Figure 8: Results of the Signorini problem obtained by the stabilized predictor-corrector method with $C = 0.5$, $\beta_s = 1e4$, optimal setting of β_m, for lumped (above), averaged (middle) and consistent (below) mass matrix: Balance of energy in time (on the left), the time history of gap function (in the middle), the time history of contact force (on the right).

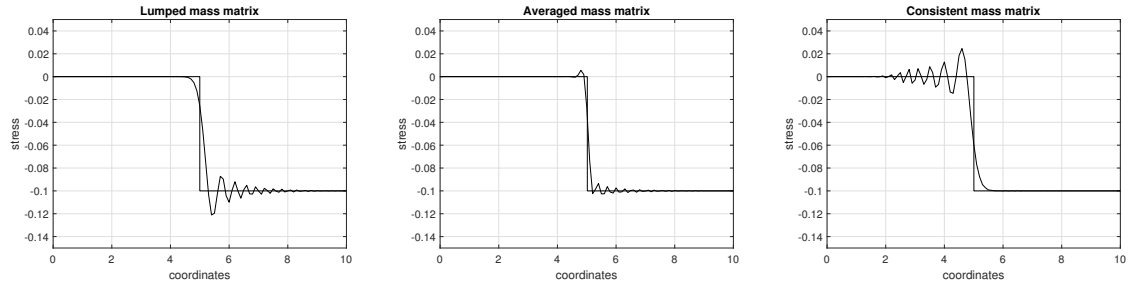

Figure 9: Stress distributions at the time $t = 0.5$ $[s]$ as results of the Signorini problem obtained by the stabilized predictor-corrector scheme with $C = 0.5$, $\beta_s = 1e4$, optimal setting of β_m, lumped (left), averaged (middle) and consistent (right) mass matrices. The analytical solution of wave propagation is attached.

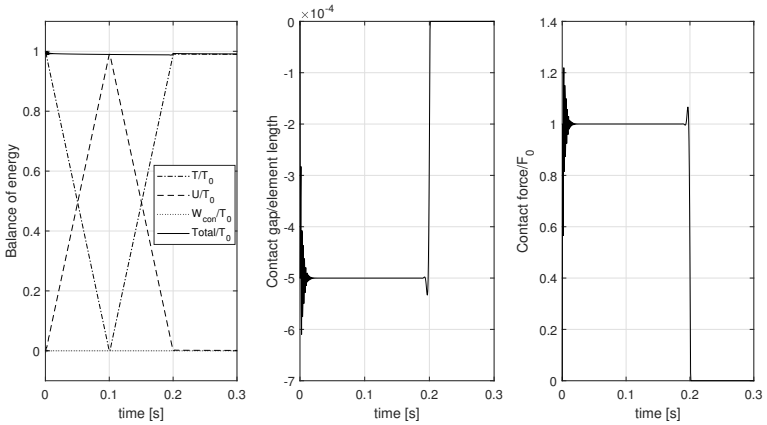

Figure 10: Results of the Signorini problem obtained by the stabilized Park method with $C = 0.5$, $\beta_s = 1e4$, optimal setting of β_m, for lumped mass matrix.

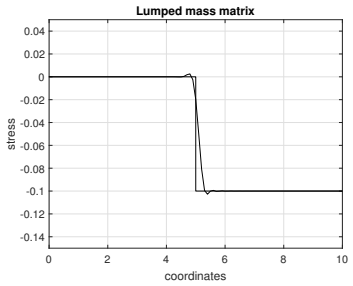

Figure 11: Stress distribution at the time $t = 0.5$ $[s]$ as results of the Signorini problem obtained by the stabilized Park method with $C = 0.5$, $\beta_s = 1e4$, optimal setting of β_m, lumped mass matrix.

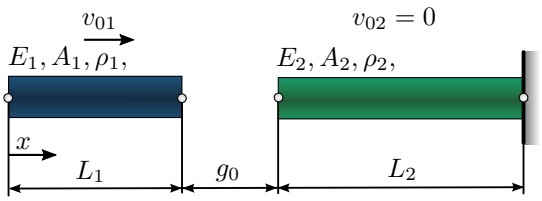

Figure 12: A scheme of an one-dimensional impact of two bars with different lengths.

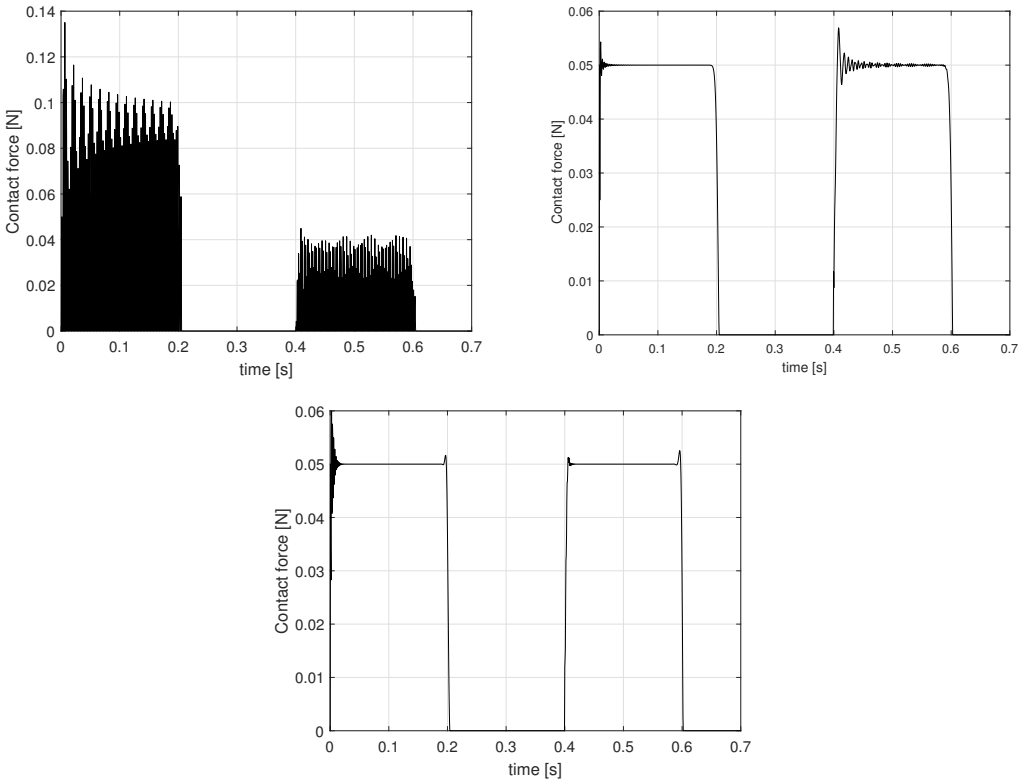

Figure 13: Time history of contact force for impact of two bars with different lengths - CD (left), the stabilized predictor-corrector scheme (middle) and Park (right) method with Courant number $C = 0.5$, $\beta_s = 1e4$, optimal β_m, lumped mass matrix.